JOURNAL OF SOLID STATE CHEMISTRY **74**, 377–384 (1988)

$Na_4Nb(PO_4)_3$, a Material with a Reversible Crystal–Glass Transformation: Structural and Optical Comparison

A. EL JAZOULI, C. PARENT, J. M. DANCE, G. LE FLEM, AND P. HAGENMULLER

Laboratoire de Chimie du Solide du CNRS, Université de Bordeaux I, 351, cours de la Libération, 33405 Talence Cedex, France

AND J. C. VIALA

Laboratoire de Physico-Chimie Minérale, Université de Lyon I, 43, Boulevard du 11 nov. 1918, 69621 Villeurbanne, France

Received September 21, 1987; in revised form December 22, 1987

The phosphate $Na_4Nb(PO_4)_3$ exhibits a reversible crystal–glass phase change. Raman and optical investigations give evidence of the similarity between the covalent skeleton of the Nasicon-like crystalline phosphate and the network of the glass. Both types of materials contain octahedral NbO_6 groups with various Nb–O lengths. It is shown for the neodymium-doped glasses that these structural features induce a strong self concentration quenching of the Nd^{3+} emission. © 1988 Academic Press, Inc.

I. Introduction

The Na_2O–Nb_2O_5–P_2O_5 system exhibits a large vitreous domain including the glass with molar composition $4Na_2O$, Nb_2O_5, $3P_2O_5$ which will be henceforth called NaNbP 413 (*1*). The crystallization of this glass leads to a Nasicon-type phosphate with the same composition, which will be represented by the formula $Na_4Nb(PO_4)_3$ (*2*). The Nasicon structure initially described by Hagman and Kierkegaard (*3*) for the $NaA_2(PO_4)_3$ phosphates (A = Ti, Zr, Ge) consists of a three-dimensional lattice built up by PO_4 tetrahedra sharing corners with AO_6 octahedra.

The sodium site of the $NaA_2(PO_4)_3$ oxides is a distorted octahedron formed by two triangular faces of neighboring AO_6 octahedra located along the c-axis of the hexagonal cell: this site is usually called M_1. In $Na_4Nb(PO_4)_3$, the A sites are equally occupied by niobium and sodium atoms; the remaining three sodium atoms are distributed in the M_1 sites and within the 3D network in sites usually called M_2 (*2*).

The crystal–glass transformation pointed out for the latter compound (*1*) involves a similarity between the skeleton of $Na_4Nb(PO_4)_3$ and the network of vitreous NaNbP 413. In the present approach we compare the structures of both types of materials—

0022-4596/88 $3.00

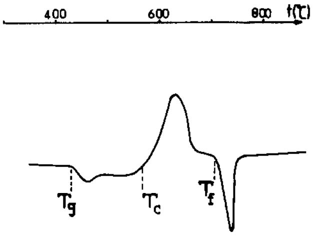

FIG. 1. DTA curves for the NaNbP 413 glass.

the crystal and the glass—using various complementary techniques such as optical, Raman, and ESR spectroscopies. On the other hand NaNbP 413 is a sodium ion conductor, which supposes weak bonding at the sodium sites. Therefore it was worthwhile to substitute Nd^{3+} for Na^+ in order to estimate the self quenching intensity of the $^4F_{3/2}$ emission.

II. Experimental

Undoped and Nd^{3+}-doped NaNbP 413 glasses have been prepared according to a procedure previously described (*1*). From the DTA curve reported in Fig. 1, the temperatures of vitreous transition, recrystallization, and melting of the undoped glass were found at slow heating to be 430, 570, and 710°C, respectively.

Recrystallization of the undoped glass resulted in the compound $Na_4Nb(PO_4)_3$. Melting and slow cooling leads reversibly to the NaNbP 413 glass.

Recrystallization of neodymium-doped glasses—$(1 - x)$NaNbP 413, xNd_2O_3—gave rise to a mixture of two compounds, $Na_4Nb(PO_4)_3$ and $NdPO_4$. The observed $NdPO_4$ rate in the two-phase mixture increases with rising neodymium content in the glasses.

$Na_4Nb(PO_4)_3$ was obtained in air from a stoichiometric mixture of Na_2CO_3 (Merck 99.5%), Nb_2O_5 (Merck Optipur), and $(NH_4)_2HPO_4$ (Merck 99.5%), according to the following equation:

$$4Na_2CO_3 + Nb_2O_5 + 6(NH_4)_2HPO_4 \rightarrow 2Na_4Nb(PO_4)_3 + 12NH_3\nearrow + 9H_2O\nearrow + 4CO_2\nearrow .$$

The reagents were first heated at 200°C for 2 hr, then at 400°C for 4 hr, and finally at 650°C for 15 hr.

Diffuse reflectance and absorption measurements were carried out at room temperature using a Cary 17 spectrophotometer. For the Raman spectra recording a Jobin–Yvon Raman spectrometer was coupled with a Spectra Physics Model 2560 Ar laser. Samples were pressed pellets ($\emptyset$ = 13 mm, th. = 1.5 mm) prepared from powders of either ground glasses or crystallized materials.

The lifetime of the Nd^{3+} $^4F_{3/2}$ level was deduced from the $^4F_{3/2} \rightarrow {}^4I_{11/2}$ fluorescence decay after a pulsed nonselective excitation in the $^4G_{5/2}$ and $^4G_{7/2}$ levels. The source was a Rhodamine 590 solution excited by a nitrogen laser and the Varian VPM 159A photomultiplier was connected to a PAR M162 boxcar averager.

The ESR spectra were recorded using a Bruker ER 200tt spectrometer working at *X*-band, associated with an Oxford Instrument continuous flow cryostat allowing operating at any temperature between 4.2 and 300 K.

III. Optical Absorption

The diffuse reflectance spectra of NaNbP 413 and $Na_4Nb(PO_4)_3$ are compared in Fig. 2 with those of $NaNbO_3$ and α-$NbPO_5$. The strong absorption thresholds observed correspond to an electronic transfer which can be schematized:

$$O^{2-}(2p^6) + Nb^{5+}(4d^0) \rightarrow O^-(2p^5) + Nb^{4+}(4d^1t_{2g}).$$

These thresholds are all located at high energies and occur in the following sequence: $NaNbO_3$ (E = 3.29 eV), α-$NbPO_5$ (E = 3.49 eV), $Na_4Nb(PO_4)_3$ (E = 3.70 eV), NaNbP 413 (E = 3.76 eV).

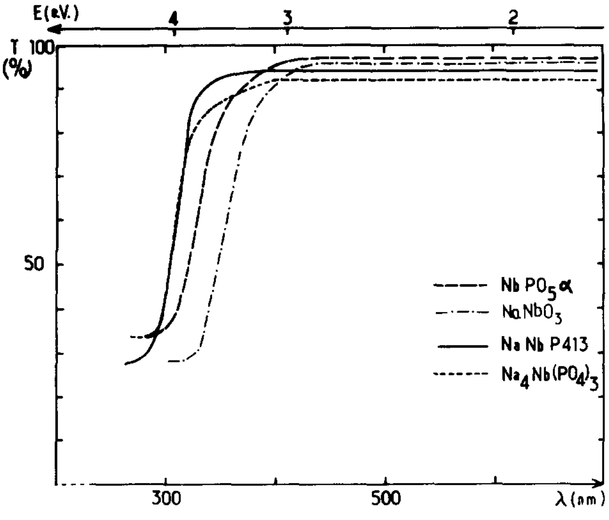

FIG. 2. Comparison of the diffuse reflectance spectra of NaNbP 413 and $Na_4Nb(PO_4)_3$ with those of $NaNbO_3$ and α-$NbPO_5$.

In the perovskite-type niobate $NaNbO_3$ (*4*) the NbO_6 octahedra share only corners. The structure of α-$NbPO_5$ contains chains of corner-sharing NbO_6 octahedra linked together by PO_4 tetrahedra (*5*). The increasing *E* values result from the more ionic character of the Nb–O bonds, which is strengthened by competition with the strongly covalent PO_4 groups.

The slight difference between the E values of crystallized $Na_4Nb(PO_4)_3$ and vitreous NaNbP 413 reveals a high degree of similarity for the Nb–O bonds in both types of materials. The small increase observed for the glass involves slightly strengthened covalency.

IV. Raman Scattering

The Raman spectra of NaNbP 413 and $Na_4Nb(PO_4)_3$ are reported in Fig. 3. Their band maxima are listed in Tables I and II. The glass spectrum is approximately the envelope of the crystallized phosphate spectrum.

For the phosphate glass the bands at 900, 630, 450, and 260 cm^{-1} may be assigned to the Nb–O bonds in octahedral sites (*6, 7*). The strongest band at 900 cm^{-1} is associated with short niobium-oxygen distances ($d \simeq 1.70$ Å). In the high energy region, i.e., above 1000 cm^{-1}, the observed bands characterize the symmetrical and antisymmetrical P–O stretching vibrations (*8*).

The large number of lines recorded in the $Na_4Nb(PO_4)_3$ spectrum does not allow a complete assignment, due to lack of a detailed crystal structure determination.

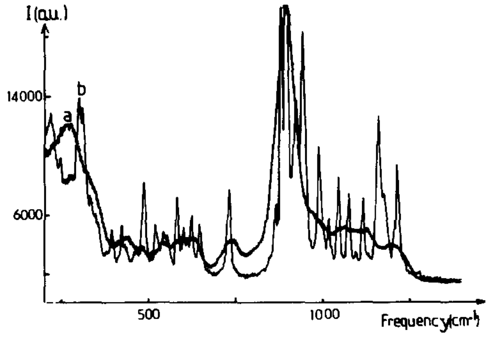

FIG. 3. Raman spectra of NaNbP 413 (a) and $Na_4Nb(PO_4)_3$ (b).

TABLE I

BAND LOCATIONS AND TENTATIVE ASSIGNMENTS FOR THE NaNbP 413 GLASS

Band locations (cm^{-1})	Assignments
1202	γ_{P-O}
1131	
1047	
902	γ_{Nb-O} (short Nb–O distances)
740	γ_{Nb-O} (medium Nb–O distances) + $\delta_{(O-P-O)}$
628	
597	
543	
517	$\delta_{(O-P-O)} + \delta_{(O-Nb-O)}$
489	
437	
333	
268	

However, some qualitative remarks can be formulated:

(i) The lines above 950 cm^{-1} characterize the stretching modes of PO_4 units. The energy values are close to those published by Nagai *et al.* (*9*) for the related $Na_xNb_{1-x}Zr_{1+x}(PO_4)_3$ solid solution.

(ii) The lines between 950 and 865 cm^{-1} can be assigned to the Nb–O stretching mode with short Nb–O distances. The high intensity line at 897 cm^{-1} is consistent with a Nb–O distance of about 1.70 Å (*6*).

(iii) The lines between 733 and 583 cm^{-1} can be associated with the Nb–O stretching modes for longer Nb–O bonds, and also with the O–P–O bending modes (*10*).

(iv) The particularly large number of narrow lines observed over the whole spectrum results from the distortion of the PO_4 groups which are surrounded by ions with different charges and sizes: Na^+ and Nb^{5+}.

In conclusion the Raman scattering investigation illustrates the similarities in the arrangement of the PO_4 and NbO_6 groups for the crystal and the glass.

V. ESR Study

Blue samples can be obtained for both vitreous and crystalline materials, corresponding to the chemical formula $Na_{4+y}Nb(PO_4)_3$ ($y \simeq 0.02$). The chromophoric groups have been identified by an ESR study.

V.1. Material Elaboration

Blue glasses were prepared from a stoichiometric mixture of Na_2CO_3, Nb_2O_5, $NaPO_3$, and Nb according to the reaction:

$$5(1+y)Na_2CO_3 + (5-y)Nb_2O_5 + 2yNb + 30NaPO_3 \rightarrow 10Na_{4+y}Nb(PO_4)_3 + 5(1+y)CO_2\uparrow.$$

This reaction has been carried out in an alu-

TABLE II

BAND LOCATIONS AND TENTATIVE ASSIGNMENTS FOR $Na_4Nb(PO_4)_3$

cm^{-1}	Assignment	cm^{-1}	Assignment
1277 vl	ν_{P-O}	733 l	ν_{Nb-O} medium Nb–O distances + $\delta_{(O-P-O)}$
1217 m		649 l	
1186 sh		625 l	
1177 sh		613 vl	
1163 m		602 vl	
1118 l		583 l	
1098 vl		545 vl	$\delta_{(O-P-O)} + \delta_{(O-Nb-O)}$
1077 l		522 vl	
1047 l		488 l	
1020 l		469 vl	
1000 sh	ν_{Nb-O} short Nb–O distances	439 vl	
993 m		427 vl	
947 s		396 l	
927 s		345 sh	
897 vs		332 l	
883 s		311 s	
865 l		301 s	
		247 sh	
		218 s	

Note. vl, very low; l, low; m, medium; s, strong; vs, very strong; sh, shoulder.

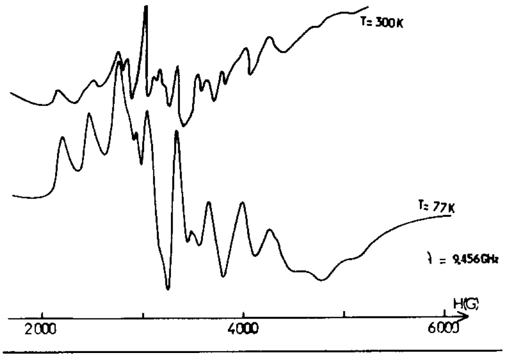

FIG. 4. ESR spectra of NaNbP 4.02 1 3.

mina vessel under an argon stream. The temperature was progressively raised from 25 to 800°C and kept at that level for 30 min. After quenching down to room temperature under argon, a blue glass was obtained.

Annealing of this glass at 560°C in a silica tube sealed under vacuum gave rise to a blue crystallized material, the X-ray spectrum of which was identical to that of $Na_4Nb(PO_4)_3$.

V.2. ESR Investigation of the Blue Glass NaNbP 4.02 1 3

The variation of the ESR spectrum of the glass from 77 to 300 K can be observed in Fig. 4. This spectrum exhibits an anisotropic structure, which can be attributed to a niobium 4+ ion. The hyperfine structure resulting from the interaction between the unpaired $4d^1$ electron and the niobium nucleus spin ($I = \frac{9}{2}$), shows two groups of 10 lines, leading to the following ESR parameters: $g_\parallel = 1.846$, $g_\perp = 1.851$, $|A_\parallel| = 320$ G, $|A_\perp| = 156$ G.

This type of spectrum is very close to those obtained for radiation-induced centers in Na_2O–Nb_2O_5–SiO_2 glasses ($|A_\parallel| = 325$ G, $|A_\perp| = 164$ G) (*11*). The strong anisotropy of hyperfine couplings is similar to that found for the vanadyl group. Therefore, we can label this chromophoric niobium center as a "niobyl" group.

The electronic configuration of Nb^{4+} is $4d^1$. Assuming a local C_{4v} symmetry, which often occurs at least roughly for the vanadyl unit, the unpaired electron occupies the molecular orbital b_{2g} (d_{xy}), which can be written schematically

$$b_{2g} = \alpha b_{2g} + \beta,$$

where β is a linear combination of ligand atomic orbitals and α the square root of the occupancy probability of the $4d_{xy}$ atomic orbital by the electron (*12*).

$A_\parallel$ and $A_\perp$ are related to the function $P = \alpha^2 P_o$, which characterizes the anisotropic coupling ($P_o = 305.4$ G for the free ion), according to equations:

$$A_\parallel = A_{\text{isotr.}} - \frac{4}{7}P \quad \text{and} \quad A_\perp = A_{\text{isotr.}} + \frac{2}{7}P.$$

For the investigated glass $P = 191$ and $\alpha^2 = 0.63$. This low value assumes a significant but not surprising electronic transfer of the electron from the metal to the ligand. This result confirms also the existence of very short niobium–oxygen bonds within the NbO_6 octahedra.

V.3. ESR Investigation of the Crystalline Compound $Na_{4.02}Nb(PO_4)_3$

The spectrum of the crystallized compound differs clearly from that of the glass (Fig. 5). It can be observed only at low temperature and shows a 10-line isotropic structure, each component of which widens

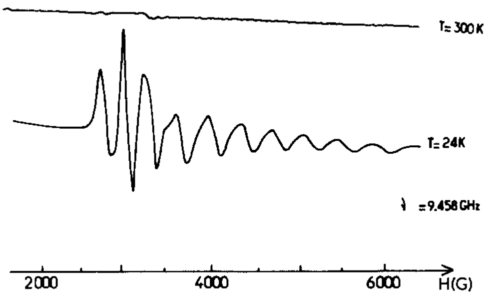

FIG. 5. ESR spectra of $Na_{4.02}Nb(PO_4)_3$.

TABLE III

CHARACTERIZATION OF THE $^4F_{3/2} \rightarrow {}^4I_{11/2}$ EMISSION FOR THE NaNbP 413 : Nd^{3+} GLASSES

	(1 − x) NaNbP 413 − x Nd_2O_3 glasses							
Molar concentration x	0	0.007	0.014	0.027	0.0402	0.053	0.065	0.077
Density (±0.02)	2.88	2.90	2.92	2.94	2.96	2.98	3.00	3.02
Neodymium concentration N (10^{20} ions × cm^{-3})	0	0.52	1.05	2.05	3.08	4.11	5.09	6.10
$\tau_N(^4F_{3/2} \rightarrow {}^4I_{11/2})$ i.e., measured lifetime (μ_s)		321	322	290	232	193	180	168

when the magnetic field increases. The separation between the first two peaks is measured as 300 G while the separation between the final two peaks on the high field side is found to be 430 G. Taking the second-order correction into account, we found $g_{\text{isotr.}} = 1.551$ and $|A_{\text{isotr.}}| = 375$ G at 24 K. This high value compared to the equivalent one found for the glass ($\frac{1}{3}A_{\parallel} + \frac{2}{3}A_{\perp} = -221$ G) implies a weaker electronic transfer. Thus the chromophor of the crystalline material is clearly the Nb^{4+} ion.

Observation of an isotropic hyperfine structure for such a weak g value at low temperature is in agreement with recent results published by Amies *et al.* (*13*) for the similar Ti^{3+} ion ($3d^1$). At very low temperature these authors assume a dynamic Jahn–Teller effect provided by a vibronic coupling between the ^2E_g and $^2T_{2g}$ states, inducing a large reduction of the g factor which can vary between 2 and 0.5. Within the scope of this model, where the Jahn–Teller stabilization is equal to the lattice vibration energy, the g value that we find (1.55) is identical to that obtained for $Na_{4.02}Nb(PO_4)_3$.

VI. Neodymium Self Concentration Quenching for the Nd-Doped Glasses

The investigated glasses had the compositions given in Table III. Whatever the neodymium concentration the maximum of the $^4F_{3/2} \rightarrow {}^4I_{11/2}$ emission occurs at λ_m = 1056 nm and the effective bandwidth is about 24 nm.

The emission intensity has been calculated by integrating the band corresponding to the $^4F_{3/2} \rightarrow {}^4I_{11/2}$ transition. The results illustrated in Fig. 6 show a decrease of the emission for concentrations exceeding 2.5 × 10^{20} Nd^{3+} = ions · cm^{-3}, which characterizes a strong self concentration quenching.

In order to provide a better insight into the quenching process, decay curves of the $^4F_{3/2}$ emission have been recorded. The emission decays appeared always to be exponential, with lifetime values decreasing with increasing Nd^{3+} ion concentration (Table III).

Assuming that the lifetime τ_0 measured for low neodymium concentrations is the radiative one, the nonradiative deexcitation probability W_{NR} can be written as

$$W_{NR} = \frac{1}{\tau_0} q_n \quad \text{where} \quad q_n = \frac{\tau_0 - \tau_N}{\tau_N}$$

(τ_N is the lifetime for a neodymium concentration N).

Figure 7 shows that q_n varies approximately as the square of the activator ion concentration (slope, 1.8).

In agreement with Ref. (*14*) it can be concluded that the self quenching of neodymium emission is due to cross-relaxation between two neighboring Nd^{3+} ions A and B involving the energy transfer

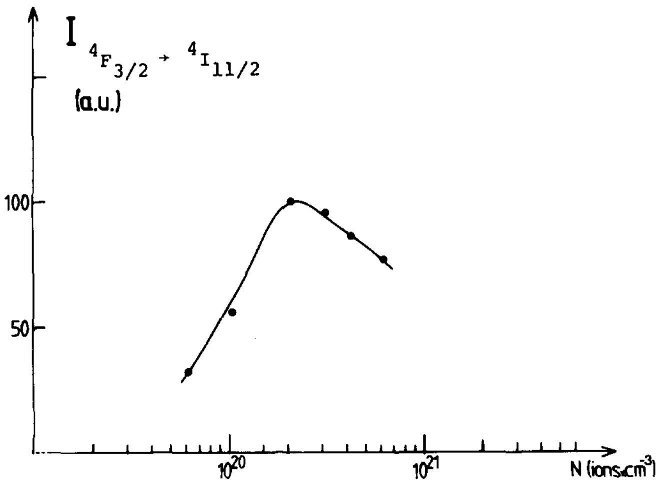

FIG. 6. Variation of the $^4F_{3/2} \rightarrow {}^4I_{11/2}$ emission intensity under constant excitation vs Nd^{3+} concentration for the NaNbP 413 : Nd^{3+}-doped glasses.

$$Nd^{3+}_{^4F_{3/2}}(A) + Nd^{3+}_{^4I_{9/2}}(B) \rightarrow 2Nd^{3+}_{^4I_{15/2}}(A + B).$$

Moreover, it is well known that the effectiveness of this process depends on the relative splitting of the $^4F_{3/2}$, $^4I_{15/2}$, and $^4I_{9/2}$ levels and consequently on the crystal field strength at the neodymium site. According to Auzel (*15*) strong self quenching must occur if the $^4I_{9/2}$ splitting ΔE_1 is higher than 470 cm^{-1}.

As the $^2P_{1/2}$ level does not split under the influence of the crystal field, the ΔE_1 value can be estimated by measuring the bandwidth corresponding to the $^4I_{9/2} \rightarrow {}^2P_{1/2}$ transition. In NaNbP 413 : Nd ΔE_1 is found to be equal to 616 cm^{-1}. This relatively high value results from the introduction of NbO_6 groups in the phosphate network. Indeed the ionicity of the Nb–O bonds induces an increase of the charge carried by the oxygen atoms and consequently of the crystal field at the rare-earth site, which becomes higher than those existing for low self concentration quenching phosphates (*14*, *15*).

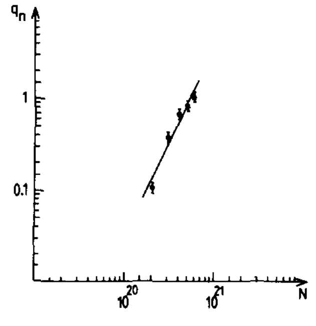

FIG. 7. Variation of the nonradiative deexcitation probability vs Nd^{3+} concentration for the NaNbP 413 : Nd^{3+} glasses.

VII. Conclusions

The $Na_4Nb(PO_4)_3$ phosphate exhibits a reversible crystal–glass phase change. The similarity of the covalent skeleton of the Nasicon-type crystalline phosphate with the network of the corresponding glass accounts for the easy transition, as pointed out by the diffuse reflectance and Raman scattering spectroscopy investigations.

Moreover Raman and ESR studies give evidence of short Nb–O bonds in the coordination polyhedron of the niobium atoms.

In neodymium-doped glasses one may assume that the presence of strongly ionic NbO_6 units within the glass network brings about a relatively high electric field at the rare-earth site and therefore induces the strong self concentration quenching observed for the neodymium emission.

References

1. A. El Jazouli, C. Parent, J. M. Dance, and G. Le Flem, *C.R. Acad. Sci. Paris Ser. 2* **303,** 1005 (1986).
2. A. El Jazouli, R. Brochu, J. C. Viala, R. Olazcuaga, C. Delmas, and G. Le Flem, *Ann. Chem. Fr.* **7,** 285 (1982).
3. L. Hagman and P. Kierkegaard, *Acta Chem. Scand.* **22,** 1822 (1968).
4. H. D. Megaw, *Acta Crystallogr. Sect. A* **24,** 589 (1968).
5. J. M. Longo and P. K. Kierkegaard, *Acta Chem. Scand.* **20,** 72 (1966).
6. E. Husson and Y. Repelin, *C.R. Acad. Sci. Paris Ser. 2* **296,** 1405 (1983).
7. G Burns, T. D. Axe, and D. F. O'Kane, *Solid State Commun.* **7,** 933 (1969).
8. Vu Ti Bich, M. Prod'Homme, M. Jouan, and N. Quy Dao, *Verres Refract.* **39**(1), 13 (1985).
9. M. Nagai, S. Fujitsh, T. Kanazawa, and H. Yanagida, *J. Mater. Sci.* **16,** 1633 (1981).
10. G. T. Stranford and R. A. Condrate, Sr., *J. Mater. Sci. Lett.* **3,** 303 (1984).
11. Y. M. Kim, D. E. Reardon, and P. J. Bray, *J. Chem. Phys.* **48**(8), 3396 (1968).
12. B. A. Goodman and J. B. Raynor, *Adv. Inorg. Chem. Radiochem.* **13,** 135 (1970).
13. R. A. Amies, S. Kremer, and D. Reinen, *Inorg. Chem.* **24,** 2751 (1985).
14. F. Auzel, *Mater. Res. Bull.* **14,** 223 (1979).
15. F. Auzel, *in* "Radiationless Processes" (Di Bartolo, Ed.), Plenum, New York/London (1980).